COMPDYN 2015
5th ECCOMAS Thematic Conference on
Computational Methods in Structural Dynamics and Earthquake Engineering
M. Papadrakakis, V. Papadopoulos, V. Plevris (eds.)
Crete Island, Greece, 25–27 May 2015

DYNAMIC ANALYSIS OF TRAIN-BRIDGE SYSTEM SUBJECTED TO EARTHQUAKE ACTION CONSIDERING TOPOGRAPHIC EFFECTS

Hong Qiao[1], He Xia[1], Xianting Du[1] and Yong Nan[1]

[1] School of Civil Engineering, Beijing Jiaotong University
Shangyuancun 3#, Haidian District, Beijing 100044, China
E-mail: CarrieQh@163.com, hxia88@163.com, wadmdxt@163.com, nanyong582613@163.com

Keywords: train-bridge system, dynamic response, earthquake action, topographic effects, viscous- spring artificial boundary.

Abstract. *A method taking into consideration the topographic effects in dynamic analysis of a train-bridge system subjected to earthquake action is presented and the influence of topography on the seismic response of train-bridge system is studied. Based on the theory of viscous-spring artificial boundary, a 3-D finite element model for the site considering topographic effect is established by using the ANSYS. The procedure of wave input is realized by transforming the seismic time history into equivalent loads acting on the artificial boundary, by means of which the seismic time histories at the supports of bridge are obtained. The dynamic model for a train-bridge system subjected to multi-support seismic excitations is established, in which the velocity and displacement time histories of earthquake waves are exerted on the bridge supports. With a train passing through a 480m bridge as a case study, the dynamic response of the train-bridge system under earthquakes considering local topography of the site is analyzed, and compared with those without considering the topographic effect. The results show that when the topographic effect is considered, the dynamic response of the train-bridge system changes on the peak value as well as the time of the peak appearance, showing that it is necessary to consider the topographic effect in dynamic analysis of train-bridge system under earthquakes.*

1 INTRODUCTION

In recent years, the railway transportation has gained rapid development. To ensure the safety and stability of running trains, more and more bridges including viaducts are built, which inevitably increases the possibility of trains on bridges when an earthquake occurs. As a result, the problem of train-bridge interaction during an earthquake has become a research hotspot recently [1-7].

In China, among the extensive railways which have already been built or are under construction, many of them are located in the southwestern regions with mountainous site topographies. On the other hand, these regions are also seismic zones susceptible to earthquakes. The 2008 Wenchuan Earthquake occurring in Sichuan Province is a typical example which caused a wide range of damages on different types of railway bridges [8]. Therefore, it is of significance to study the seismic response of bridges located at these regions. In seismic design, it has been long recognized that the local topography has a significant effect on the amplitude of ground motion during earthquakes. Celebi performed site-response experiments 5 months after the Chile earthquake (Central Chile, M7.8) and found that structures located at ridges suffer more intensive damage than other places [9]. Jibson measured the acceleration peaks across a ridge in Japan and the measurements showed that compared with the base, there was an amplification at the crest varying from 1.8 to 5.5 [10]. In the 2008 Wenchuan Earthquake, the complex topography may be one of the main factors leading to the collapse of the Baihua Bridge as well as the Miaoziping Bridge [11]. Lee et al. [12] investigated the effects of high-resolution surface topography on seismic ground motion and found that the amplification of ground motion mainly occurs at the tops of hills and ridges while the valleys and flat-topped hills experience lower levels of ground shaking. There are also many other papers discussing the topographic effects on the peak of ground motion and on the seismic response of bridges [13-18]. All these publications indicated the necessity of considering the topographic effects in seismic design, but few of them discussed the seismic response of train-bridge coupling system considering this aspect.

In this regard, this paper presents a method for dynamic analysis of train-bridge system subjected to earthquake action considering local topography. In this method, the train-bridge system consists of the bridge subsystem and the train subsystem. The two subsystems are established by mode superposition method and rigid-body dynamics method, respectively and the Newmark-β method is used to solve the dynamic interaction. To take the topographic effects into account, a 3-D analytical model of local site based on the theory of viscous-spring artificial boundary and finite element method is established. The process of wave input is realized by transforming the seismic time history into equivalent loads acting on the artificial boundary, by means of which the seismic time history at each support of bridge can be obtained. Then the dynamic analysis of a train-bridge system subjected to multi-support seismic excitations is carried out, in which the velocity and displacement time histories of seismic excitations obtained by the above method are exerted on the bridge supports. A train passing through a 480m continuous bridge is taken as a case study and the dynamic response of train-bridge system under earthquakes considering local topography are analyzed.

2 SEISMIC EXCITATIONS CONSIDERING LOCAL TOPOGRAPHY

To realize the procedure of earthquake wave propagating in the soil of local site, the finite element method is an efficient way. A key step of this method is to extract a finite domain from the infinite soil medium, which means a verified virtual artificial boundary able to absorb the energy of the scattering waves is necessary. The 3D viscous-spring artificial boundary proposed by Liu [19] not only satisfies the above criterion but also has advantages of high

numerical precision, adequate stability and convenience in application. Therefore, in this analysis, the 3D viscous-spring artificial boundary is used when establishing the model of local site.

2.1 Input method of seismic wave

The problem of how to input the seismic wave can be converted into a wave source problem [20], which means the input motion is converted into equivalent loads acting on the artificial boundary to simulate the procedure of seismic wave input. The equivalent loads F_{BN} and F_{BT}, respectively in the normal and tangential directions, can be expressed as follows.

$$F_{BN} = \sigma_0\left(x_B, y_B, t\right) + C_{BN}\dot{u}_0\left(x_B, y_B, t\right) + K_{BN}u_0\left(x_B, y_B, t\right) \tag{1}$$

$$F_{BT} = \tau_0\left(x_B, y_B, t\right) + C_{BT}\dot{v}_0\left(x_B, y_B, t\right) + K_{BT}v_0\left(x_B, y_B, t\right) \tag{2}$$

where $u_0(x, y, t)$ and $v_0(x, y, t)$ are the normal and tangential displacement of the incident wave, respectively; $\sigma_0(x, y, t)$ and $\tau_0(x, y, t)$ are the normal and tangential stress determined by $u_0(x, y, t)$ and $v_0(x, y, t)$, respectively; x_B and y_B are the node coordinates of the artificial boundary; K_{BN}、K_{BT}、C_{BN}、C_{BT} are the spring coefficients and damping coefficients of the normal and tangential springs respectively, the values of which can be determined according to the following equations [19],

$$\left.\begin{aligned} K_{BN} &= \frac{\alpha_N G}{R} \\ K_{BT} &= \frac{\alpha_T G}{R} \\ C_{BN} &= \rho c_p \\ C_{BT} &= \rho c_s \end{aligned}\right\} \tag{3}$$

where α_N and α_T are the coefficients in the normal and tangential directions respectively, which can be referred to Table 1; G is the shear modulus and ρ is the mass density of the medium, namely the solid of the local site; R is the distance between the load point and the boundary, which can be obtained approximately by simply taking the value of the perpendicular distance from the load point to the boundary.

Parameters	Value range	Recommended value
$\boldsymbol{\alpha_N}$	1.0~2.0	4/3
$\boldsymbol{\alpha_T}$	0.5~1.0	2/3

Table 1: Recommended value of α_N and α_T

2.2 Calculation of equivalent loads

Generally, the focus of an earthquake is deep and there are usually many refractions happening during the propagation process of the seismic wave, which results in the vertical incidence of the earthquake wave when it arrives at the earth surface. Therefore, in this analysis, the seismic wave is assumed to be a plane incident one travelling perpendicularly to the ground surface. The time histories of the incident plane P wave and S wave are $u_P(t)$ and $u_S(t)$ respectively. The *x*-*y* plane of the rectangular coordinate system is parallel to the bottom of the model and the *z*-axis points to the finite domain, as shown in Figure1.

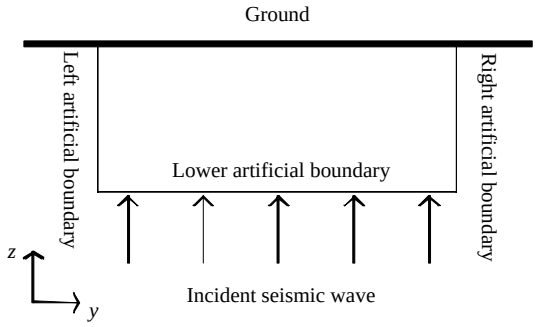

Figure1: Vertical incidence model of seismic wave

Assuming the incident S wave vibrates along the *x*-axis, the equivalent loads acting on each node of the artificial boundary can be obtained based on the wave propagation law and the stress state of the wave field [21], namely,

(1) Under the condition of incident P wave:

$$f_z^{-z}(t) = A\left[K_{\mathrm{BN}}u_{\mathrm{p}}(t) + C_{\mathrm{BN}}\dot{u}_{\mathrm{p}}(t) + \rho c_{\mathrm{p}}\dot{u}_{\mathrm{p}}(t)\right] \tag{4}$$

$$f_x^{-x}(t) = A\lambda\left[\dot{u}_{\mathrm{p}}(t-\Delta t_1) - \dot{u}_{\mathrm{p}}(t-\Delta t_2)\right]/c_{\mathrm{p}} \tag{5}$$

$$f_z^{-x}(t) = A[K_{\mathrm{BT}}u_{\mathrm{p}}(t-\Delta t_1) + C_{\mathrm{BT}}\dot{u}_{\mathrm{p}}(t-\Delta t_1) + K_{\mathrm{BT}}u_{\mathrm{p}}(t-\Delta t_2) + C_{\mathrm{BT}}\dot{u}_{\mathrm{p}}(t-\Delta t_2)] \tag{6}$$

$$f_y^{-y}(t) = -f_x^{+x}(t) = -f_y^{+y}(t) = f_x^{-x}(t) \tag{7}$$

$$f_z^{-y}(t) = f_z^{+x}(t) = f_z^{+y}(t) = f_z^{-x}(t) \tag{8}$$

(2) Under the condition of incident S wave:

$$f_x^{-z}(t) = A\left[K_{\mathrm{BT}}u_{\mathrm{s}}(t) + C_{\mathrm{BT}}\dot{u}_{\mathrm{s}}(t) + \rho c_{\mathrm{s}}\dot{u}_{\mathrm{s}}(t)\right] \tag{9}$$

$$f_x^{-x}(t) = A[K_{\mathrm{BN}}u_{\mathrm{s}}(t-\Delta t_3) + C_{\mathrm{BN}}\dot{u}_{\mathrm{s}}(t-\Delta t_3) + K_{\mathrm{BN}}u_{\mathrm{s}}(t-\Delta t_4) + C_{\mathrm{BN}}\dot{u}_{\mathrm{s}}(t-\Delta t_4)] \tag{10}$$

$$f_z^{-x}(t) = A\rho c_{\mathrm{s}}\left[\dot{u}_{\mathrm{s}}(t-\Delta t_3) - \dot{u}_{\mathrm{s}}(t-\Delta t_4)\right] \tag{11}$$

$$f_x^{+x}(t) = f_x^{-x}(t) \tag{12}$$

$$f_z^{+x}(t) = -f_z^{-x}(t) \tag{13}$$

$$f_x^{-y}(t) = A[K_{\mathrm{BT}}u_{\mathrm{s}}(t-\Delta t_3) + C_{\mathrm{BT}}\dot{u}_{\mathrm{s}}(t-\Delta t_3) + K_{\mathrm{BT}}u_{\mathrm{s}}(t-\Delta t_4) + C_{\mathrm{BT}}\dot{u}_{\mathrm{s}}(t-\Delta t_4)] \tag{14}$$

$$f_x^{+y}(t) = f_x^{-y}(t) \tag{15}$$

$$\left.\begin{aligned} \Delta t_1 &= l/c_{\mathrm{p}} \\ \Delta t_2 &= (2L-l)/c_{\mathrm{p}} \\ \Delta t_3 &= l/c_{\mathrm{s}} \\ \Delta t_4 &= (2L-l)/c_{\mathrm{s}} \end{aligned}\right\} \tag{16}$$

where the subscript of each equivalent load represents the direction of the load, and the superscript represents the outer normal direction of the boundary where the node locates; Δt_1~Δt_4 represent the time delay of the incident P wave, the reflected P wave, the incident S wave and the reflected S wave, respectively; l is the distance between the node and the lower boundary; L is the distance between the lower boundary and the ground surface; A is the representative area of the node on the artificial boundary [19]; λ is the lame constant.

2.3 Realization of the artificial boundary in FE platform

Taking ANSYS as an example, the medium can be modeled with the Solid45 elements, and the springs and dampers in the viscous-spring artificial boundary can be simulated by the Combin14 elements with its one end fixed.

3 DYNAMIC ANALYSIS MODEL OF TRAIN-BRIDGE COUPLING SYSTEM SUBJECTED TO SEISMIC LOAD

The train-bridge system consists of the bridge subsystem and the train subsystem, as shown in Figure 2. A global coordinate system satisfying the right-hand rule is defined for the train-bridge system, in which the *y*-axis is taken as the longitudinal direction of the bridge and the *x*-axis is the lateral direction of the bridge. Before establishing the motion equations of these two subsystems, several assumptions are made,

(1) The train passes through the bridge with a constant speed;

(2) The seismic ground motions at all supports of the bridge are different;

(3) The seismic load only directly acts on the bridge subsystem and the influence on the train subsystem due to earthquake can be realized by the wheel-track interaction relation.

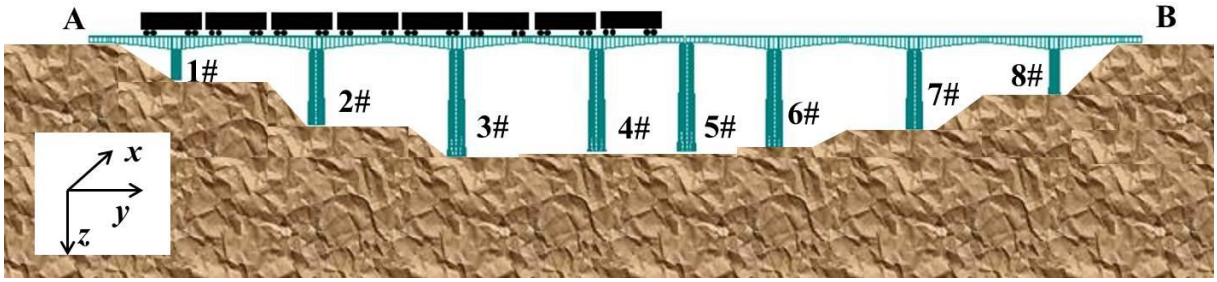

Figure 2: The bridge-train system

The train-bridge dynamic interaction during earthquakes can be described by finite element method and the motion equations of the train subsystem and the bridge subsystem can be expressed as [7]:

$$\boldsymbol{M}_{\mathrm{V}}\ddot{\boldsymbol{u}}_{\mathrm{V}}+\boldsymbol{C}_{\mathrm{V}}\dot{\boldsymbol{u}}_{\mathrm{V}}+\boldsymbol{K}_{\mathrm{V}}\boldsymbol{u}_{\mathrm{V}}=\boldsymbol{F}_{\mathrm{V,B}} \tag{17}$$

$$\begin{bmatrix}\boldsymbol{M}_{\mathrm{ss}} & \boldsymbol{M}_{\mathrm{sb}}\\ \boldsymbol{M}_{\mathrm{bs}} & \boldsymbol{M}_{\mathrm{bb}}\end{bmatrix}\begin{Bmatrix}\ddot{\boldsymbol{u}}_{\mathrm{s}}\\ \ddot{\boldsymbol{u}}_{\mathrm{b}}\end{Bmatrix}+\begin{bmatrix}\boldsymbol{C}_{\mathrm{ss}} & \boldsymbol{C}_{\mathrm{sb}}\\ \boldsymbol{C}_{\mathrm{bs}} & \boldsymbol{C}_{\mathrm{bb}}\end{bmatrix}\begin{Bmatrix}\dot{\boldsymbol{u}}_{\mathrm{s}}\\ \dot{\boldsymbol{u}}_{\mathrm{b}}\end{Bmatrix}+\begin{bmatrix}\boldsymbol{K}_{\mathrm{ss}} & \boldsymbol{K}_{\mathrm{sb}}\\ \boldsymbol{K}_{\mathrm{bs}} & \boldsymbol{K}_{\mathrm{bb}}\end{bmatrix}\begin{Bmatrix}\boldsymbol{u}_{\mathrm{s}}\\ \boldsymbol{u}_{\mathrm{b}}\end{Bmatrix}=\begin{Bmatrix}\boldsymbol{F}_{\mathrm{B,V}}\\ \boldsymbol{0}\end{Bmatrix} \tag{18}$$

where $\boldsymbol{M}$、$\boldsymbol{C}$、$\boldsymbol{K}$ are the mass, damp and stiffness matrices, respectively, $\boldsymbol{u},\dot{\boldsymbol{u}},\ddot{\boldsymbol{u}}$ are the displacement, velocity and acceleration vectors, with the subscript V representing the train subsystem, B the bridge subsystem, s the superstructure and b the base of the bridge, respectively; $\boldsymbol{F}_{\mathrm{B,V}}$ and $\boldsymbol{F}_{\mathrm{V,B}}$ are the interaction forces between the two subsystems which are determined by the wheel-track interaction relation.

From Equation (18), the equilibrium equations of the superstructure with the specified absolute displacement at the bases of the bridge can be written as:

$$\boldsymbol{M}_{\mathrm{ss}}\ddot{\boldsymbol{u}}_{\mathrm{s}}+\boldsymbol{C}_{\mathrm{ss}}\dot{\boldsymbol{u}}_{\mathrm{s}}+\boldsymbol{K}_{\mathrm{ss}}\boldsymbol{u}_{\mathrm{s}}=-\boldsymbol{K}_{\mathrm{sb}}\boldsymbol{u}_{\mathrm{b}}-\boldsymbol{C}_{\mathrm{sb}}\dot{\boldsymbol{u}}_{\mathrm{b}}-\boldsymbol{M}_{\mathrm{sb}}\ddot{\boldsymbol{u}}_{\mathrm{b}}+\boldsymbol{F}_{\mathrm{B,V}} \tag{19}$$

The term $\boldsymbol{M}_{\mathrm{sb}}$ is usually neglected and as a result, Equation (19) can be written as:

$$\boldsymbol{M}_{\mathrm{ss}}\ddot{\boldsymbol{u}}_{\mathrm{s}}+\boldsymbol{C}_{\mathrm{ss}}\dot{\boldsymbol{u}}_{\mathrm{s}}+\boldsymbol{K}_{\mathrm{ss}}\boldsymbol{u}_{\mathrm{s}}=-\boldsymbol{K}_{\mathrm{sb}}\boldsymbol{u}_{\mathrm{b}}-\boldsymbol{C}_{\mathrm{sb}}\dot{\boldsymbol{u}}_{\mathrm{b}}+\boldsymbol{F}_{\mathrm{B,V}} \tag{20}$$

where the first two terms at right side of the equation are the seismic load acting on the bridge.

Applying the mode superposition method to Equation (20), a series of mutually independent modal equations can be obtained, namely:

$$\ddot{q}_i + 2\xi_i\omega_i\dot{q}_i + \omega_i^2 q_i = \boldsymbol{\varphi}_i^T \boldsymbol{M}_{ss}\boldsymbol{R}(2\xi_i\omega_i\dot{\boldsymbol{u}}_b) + \boldsymbol{\varphi}_i^T \boldsymbol{M}_{ss}\boldsymbol{R}(\omega_i^2\boldsymbol{u}_b) + \boldsymbol{\varphi}_i^T \boldsymbol{F}_{B,V} \qquad (i=1,2,\ldots,n) \quad (21)$$

where $\boldsymbol{\varphi}_i$ and q_i are the ith normalized mode shape and generalized coordinate, ω_i and ξ_i are the ith circular frequency and damping ratio, respectively; n is the number of the modes used in the analysis; $\boldsymbol{R}$ is called displacement influence matrix, which can be obtained by the following equation:

$$\boldsymbol{R} = -\boldsymbol{K}_{ss}^{-1}\boldsymbol{K}_{sb} \quad (22)$$

Equation (17) and Equation (21) constitute the basic motion equations of the train-bridge coupling system, and on condition that the wheel-track interaction relation is known, the dynamic response of the train-bridge system can be obtained by solving the above equations by means of numerical step-by-step integration.

4 THE PROCEDURE OF TRAIN-BRIDGE DYNAMIC ANALYSIS DURING EARTHQUAKES CONSIDERING TOPOGRAPHIC EFFECTS

Based on the theory of viscous-spring artificial boundary and the finite element method-based framework for seismic analysis of train-bridge system, the overall procedure of calculating dynamic response of train-bridge system during earthquakes considering local topography can be summarized as follows:

(1) According to the conditions of local topography, establish the 3-D finite element model with viscous-spring artificial boundary;

(2) Calculate the equivalent loads acting on the boundary. If the incident wave is travelling perpendicularly to the ground surface, use Equation (4) ~ (15); if not, there are other equations which are not presented in this paper for the moment;

(3) Apply the loads obtained in step (2) on the nodes at the boundary in the finite element model established in step (1), and then the ground motions considering the local topography at each support can be obtained.

(4) With the ground motions obtained in step (3) taken as seismic excitations, analyze the seismic response of train-bridge coupling system considering topographic effects through the element method-based framework proposed above.

5 CASE STUDY

5.1 The bridge model

In order to study the dynamic response of train-bridge system subjected to seismic action considering local topography, a train passing through a 480m bridge is taken as a case study. The local topography at the bridge site can be seen in Figure 2. It is located in a valley, as a result of which the height of the piers are different. The piers are numbered from Pier #1 to Pier #8 and the abutments are expressed as A and B at the ends of the bridge. The highest pier is Pier #5, 49m in height, and the shortest is Pier #1, 13.5m in height.

The total length of bridge is 480m composed of two continuous girders and the span layout is (40+64+64+64+40)m+(40+64+64+40)m. The girders have a box section and the configurations of the section can be seen in Figure 3.

A 3-D FE model of the railway bridge is established and the beam elements are used to model the main girder and the piers. The bottoms of Pier #1 to Pier #8 are fixed and the finite

element model is shown in figure 4. The first 100 modes are used for the train-bridge dynamic analysis and the damping ratio is assumed to be 0.05 uniformly.

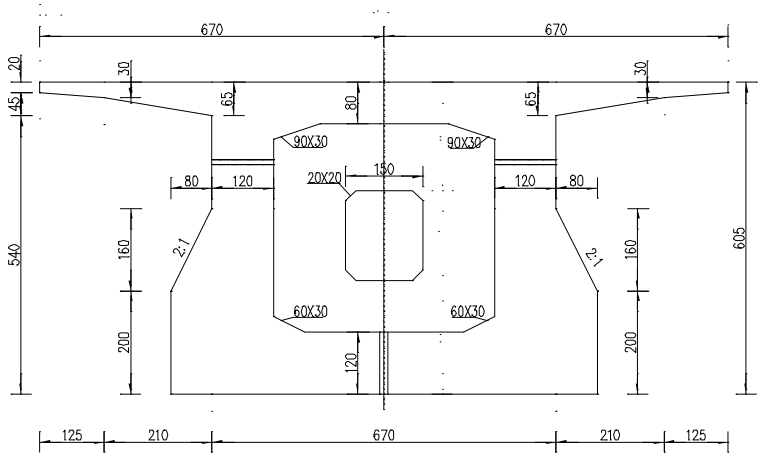

(a) Section at the top of main piers

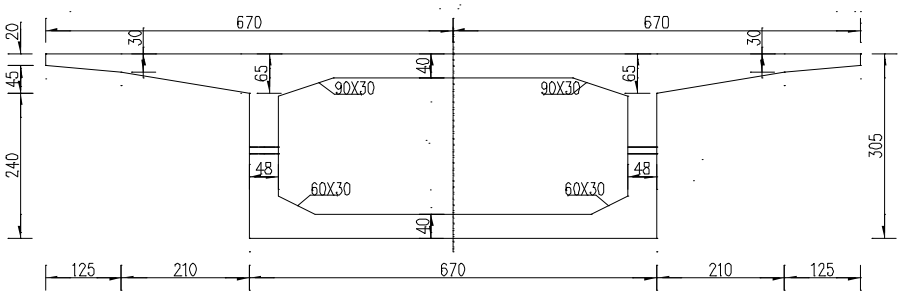

(b) Section at the mid-span

Figure 3: The girder section

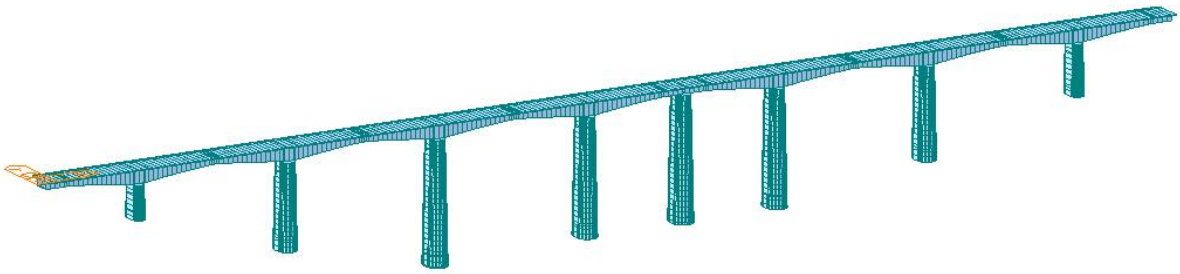

Figure 4: Finite element model of the bridge

5.2 The train model

The train used in this case study is ICE3 high-speed train with 8 vehicles. The fourth and the eighth vehicles are trailer cars and the others are motor cars. Based on the rigid body dynamics method, the model of the train subsystem is established. In this model, each vehicle is a rigid body-spring-damper discrete system and is independent from other vehicles. The mass, damping and stiffness matrices can be obtained based on the D'Alember principle and then the motion equation can be formed [5]. It is assumed that the wheel-track interaction obeys the wheel-track corresponding assumption and the German low disturbance spectra for high-speed railway are used as rail irregularities, whose vertical irregularity curve is shown in Figure 5 for reference.

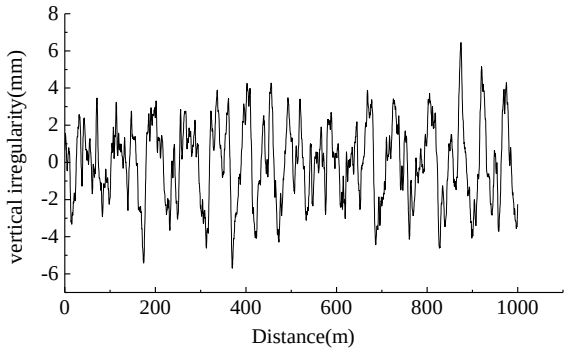

Figure 5: The vertical irregularity curve

5.3 The local topography

According to the actual conditions, the bridge is located in a valley, based on which the FE model of local topography can be established. Then according to the theory of viscous-spring artificial boundary, the equivalent loads acting on the boundary are calculated and finally the ground motions considering the local topography at each support are obtained.

A 3-D FE model of the local topography is built using a general finite element platform ANSYS [22]. The Solid45 elements are used to simulate the soil medium and the Combin14 elements are used to model the viscous-spring artificial boundary. The parameters of the local soil are shown in Table 2. The size of the element is 8m and the overall dimension of the model is 640m ×160m ×160m, which is shown in Figure 6.

Item	Parameter	Item	Parameter
Mass density	2610kg/m^3	Elasticity modulus	5GPa
Poisson's ratio	0.26	Damping ratio	0.05
Velocity of P wave	1530m/s	Velocity of S wave	871m/s

Table 2 The parameters of the soil

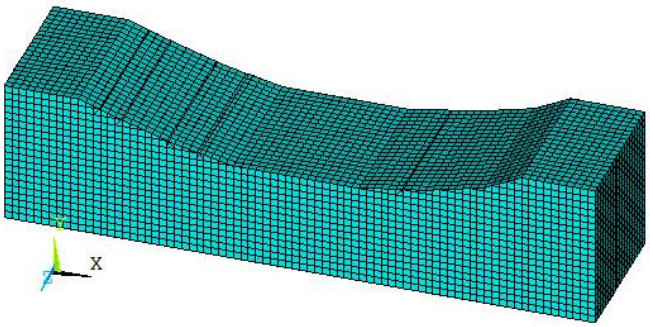

Figure 6: Finite element model of local topography

Assuming that the earthquake happens when the train just moves onto the bridge, the computational procedure for the dynamic interaction analysis of the train-bridge system during earthquakes is realized based on the above conditions.

5.4 Ground motions at each support of bridge

The ground motion time histories of the KOBE earthquake are used in this case study, as shown in Figure 7. It is assumed that the seismic waves are plane P wave and plane S wave, and the corresponding equivalent loads acting on the artificial boundary are obtained by Equations (4)~(8) and Equations (9)~(15), respectively. After the loads applied on the nodes at the boundary in the FE model, the ground motions at all supports of bridge are obtained via time-procedure analysis in ANSYS.

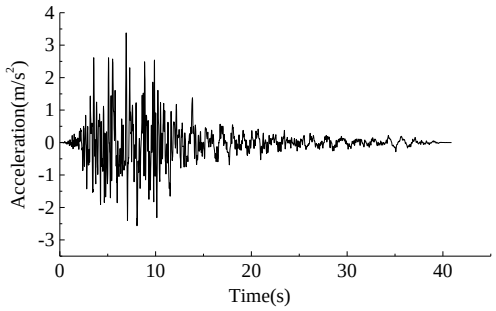

(a) Acceleration time history

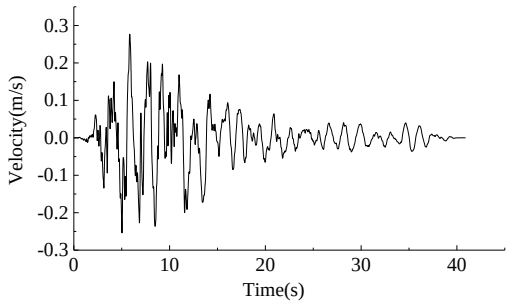

(b) Velocity time history

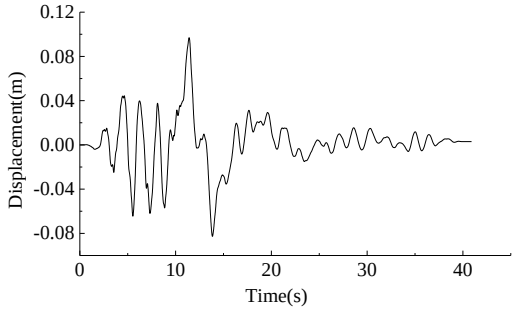

(c) Displacement time history

Figure 7: Seismic time history

The finite element model without considering local topography is also established for comparison, in which the upper surface is taken as free horizontal surface. Through the same procedure, the ground motion time histories without considering topography are obtained.

Listed in Table 3 are the RSDs (Ratios of Seismic Displacement) at different supports, where RSD is defined as the ratio of a seismic displacement maximum with considering the topography to the corresponding one without. It can be seen all the values of RSD are less than 1.0 either in horizontal or in vertical direction, meaning that the displacement maximums

decrease at all the supports after considering the topography, which corresponds to the conclusion in Reference [12].

Direction	A	1#	2#	3#	4#	5#	6#	7#	8#	B
Left(←)	0.9767	0.9540	0.9251	0.9149	0.9177	0.9154	0.9192	0.9194	0.9484	0.9773
Right(→)	0.9763	0.9521	0.9165	0.9025	0.9040	0.9017	0.8984	0.9089	0.9468	0.9766

(a) RSD in horizontal direction

Direction	A	1#	2#	3#	4#	5#	6#	7#	8#	B
Up(↑)	0.9883	0.9736	0.9510	0.9360	0.9334	0.9331	0.9352	0.9474	0.9688	0.9865
Down(↓)	0.9884	0.9711	0.9428	0.9257	0.9237	0.9232	0.9251	0.9387	0.9653	0.9862

(b) RSD in vertical direction

Table 3: RSD at different supports

5.5 Dynamic response of train-bridge system subjected to incident P wave

First, the ratios of displacement response maximums and acceleration response maximums with and without considering the topography are defined as Ratio of Displacement Response (RDR) and Ratio of Acceleration Response (RAR), respectively. Shown in Figures 8 and 9 are, respectively, the vertical acceleration and displacement time histories at mid-span of the first continuous girder at the train speed of 150km/h. It can be seen that the calculated RAR is 1.25 and the RDR is 0.94, namely for this bridge, the vertical acceleration increases while the vertical displacement decreases when the topographic effects are considered.

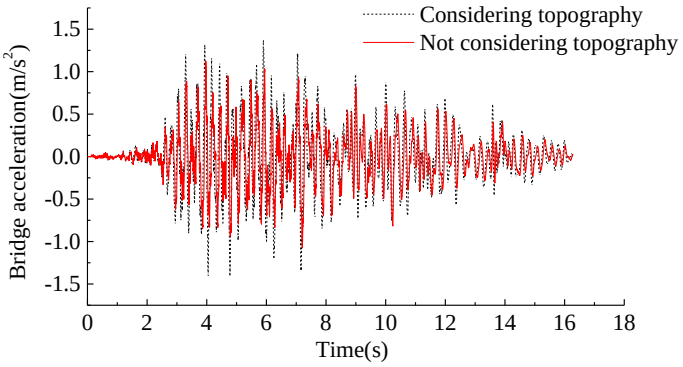

Figure8: Vertical acceleration time history of mid-span subjected to incident P wave

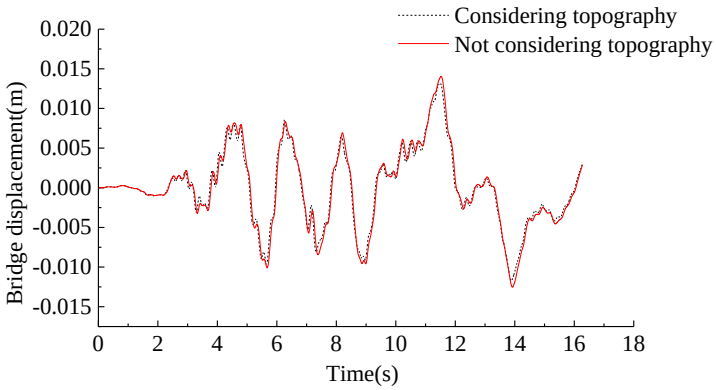

Figure9: Vertical displacement time history of mid-span subjected to incident P wave

Shown in Figures 10 and 11 are, respectively, the vertical acceleration and displacement time histories of the car-body in the first vehicle when the train speed is 150km/h. It can be seen that both the vertical acceleration and displacement of the 1st car-body increase when the topographic effects are considered, and the magnifications are 1.08 and 1.03, respectively, which demonstrates that it is necessary to take topographic effects into consideration when analyzing the dynamic response of train-bridge coupling system and assessing the running safety of trains.

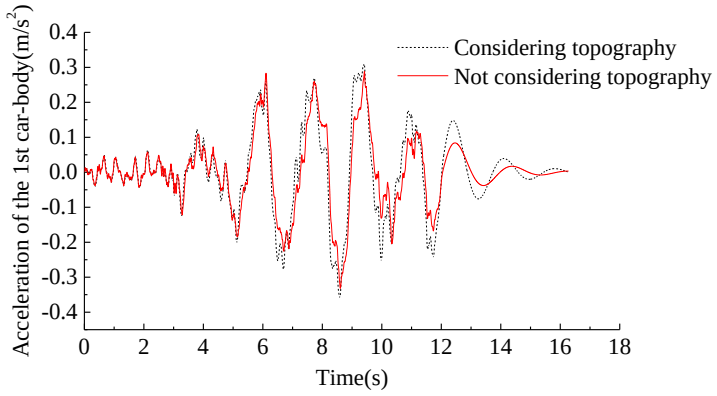

Figure 10: Vertical acceleration time history of 1st car-body subjected to incident P wave

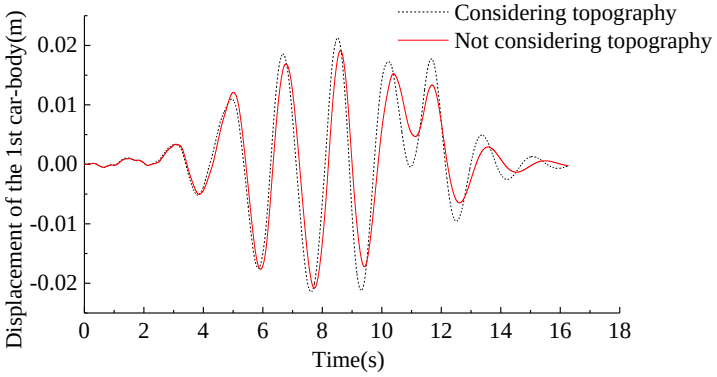

Figure 11: Vertical displacement time history of 1st car-body subjected to incident P wave

5.6 Dynamic response of train-bridge system subjected to incident S wave

Shown in Figures 12 and 13 are, respectively, the horizontal acceleration and displacement time histories at mid-span of the first continuous girder at the train speed of 150km/h. It can be seen that both the horizontal acceleration and displacement of the bridge decrease when the topographic effects are considered and RAR and RDR are about 0.92 and 0.91, respectively.

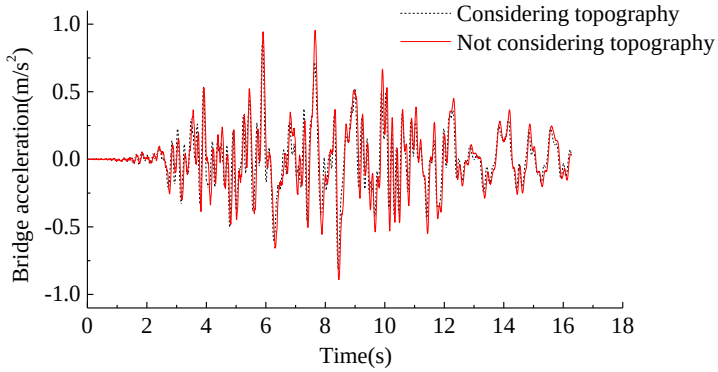

Figure 12: Horizontal acceleration time history of mid-span subjected to incident S wave

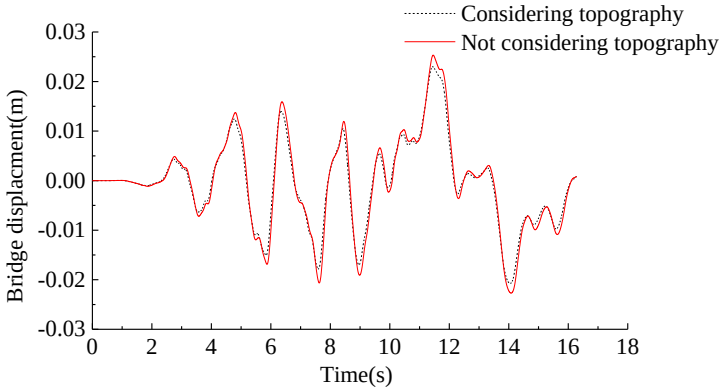

Figure 13: Horizontal displacement time history of mid-span subjected to incident S wave

Shown in Figures 14 and 15 are, respectively, the horizontal acceleration and displacement time histories of the car-body in the first vehicle when the train speed is 150km/h. Similarly, it can be seen that both the acceleration and displacement of the 1st car-body decrease when the topographic effects are considered, and the RAR and RDR of the train subsystem are about 0.80 and 0.97, respectively. The results demonstrate that the local topography of the bridge in this case study is beneficial to the coupling system.

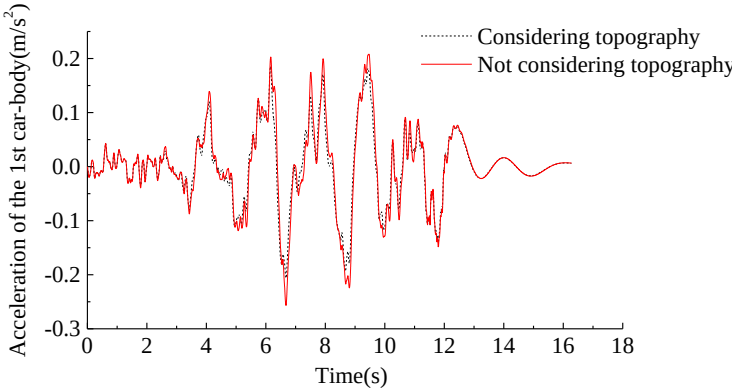

Figure 14: Horizontal acceleration time history of 1st car-body subjected to incident S wave

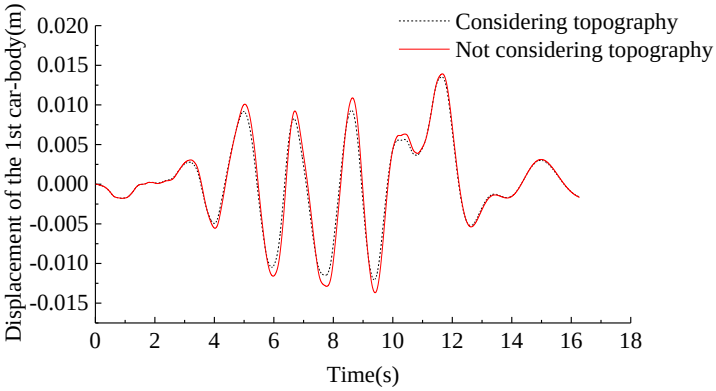

Figure 15: Horizontal displacement time history of 1st car-body subjected to incident S wave

6 CONCLUSIONS

In this paper, a method is presented to take into consideration the topographic effects in dynamic analysis of a train-bridge system subjected to multi-support seismic excitations. The influence of topography on the seismic response of train-bridge system is preliminarily studied by a case study. According to the analysis results, some conclusions can be obtained:

(1) Under the condition of incident P wave, when the topographic effects are considered, the vertical acceleration of the bridge increases while the vertical displacement decreases, and both the vertical acceleration and displacement of train increase, which demonstrate the necessity to consider the effects of local topography in bridge aseismic analysis.

(2) Under the condition of incident S wave, when the topographic effects are considered, the dynamic response of both the train subsystem and the bridge subsystem decrease, which means that in this case study, the valley helps to reduce the seismic response of train-bridge system.

(3) Different bridges may be located in different kinds of sites, as a result of which the influence of the topography on the seismic response of train-bridge coupling system may be different. Besides, there are also many other factors affecting the analysis results. However, the method proposed in this paper has its universal applicability and if necessary, it can be used in other railway bridges for seismic response analysis and running safety assessment.

ACKNOWLEDGEMENTS

This study is financially supported by the National Basic Research Program of China ("973"Project) (Grant No. 2013CB036203), the National Natural Science Foundation of China (Grant No. 51208027) and the Fundamental Research Funds for the Central Universities (Grant No. 2014YJS095)

REFERENCES

[1] T Miyamoto, H Ishida, M Matsuo, Running safety of railway vehicle as earthquake occurs. Japanese National Railway Technical Research Institute Quarterly Reports, **38(3)**, 117-122, 1997.

[2] YB Yang, YS Wu, Dynamic stability of trains moving over bridges shaken by earthquakes. Journal of Sound and Vibration, **258(1)**, 65-94, 2002.

[3] H Xia, Y Han, N Zhang, *et al*., Dynamic analysis of train-bridge system subjected to non-uniform seismic excitations. Earthquake Engineering and Structural Dynamics, **35**, 1563-1579, 2006.

[4] K Nishimura, Y Terumichi, *et al*, Experimental study on the vehicle safety by earthquake track excitation with 1/10 scale vehicle and roller rig. Journal of System Design and Dynamics, **4(1)**, 226-237, 2010.

[5] H Xia, G De Roeck, J M Goicolea, *Bridge Vibration and Controls: New Research*. New York: Nova Science Publishers Inc., 2011.

[6] X He, M Kawatani, T Hayashikawa and T Matsumoto, Numerical analysis on seismic response of Shinkansen bridge-train interaction system under moderate earthquakes. Earthquake Engineering and Engineering Vibration, **10**, 85-97, 2011.

[7] XT Du, YL Xu, H Xia, Dynamic interaction of bridge-train system under non-uniform seismic ground motion. Earthquake Engineering and Structural Dynamics, **41**, 139-157, 2012.

[8] Wang Z, A preliminary report on the great Wenchuan earthquake. Earthquake Engineering and Engineering Vibration, **7(2):** 225-234, 2008.

[9] M Celibi, Topographical and geological amplifications determined from strong-motion and aftershock records of the 3 March 1985 Chile earthquake. Bulletin of the Seismological Society of America, **88(4):** 1147-1167, 1987.

[10] R Jibson, Summary of research on the effects of topographic amplification of earthquake shaking on slope stability. US Geological Survey, Open-file Report 87-268, Menlo Park, California, 1987.

[11] GL Zhou, Canyon topography effects on seismic response of multi-support bridges. Harbin: Institute of Engineering Mechanics, China Earthquake Administration, 2010. (in Chinese)

[12] S J Lee, Y C Chan, D Konatitsch, et al., Effects of realistic surface topography on seismic ground motion in the Yangminshan region of Taiwan based upon the spectral-element method and lidar DTM. Bulletin of the Seismological Society of America, **99(2A)**, 681-693, 2009.

[13] M. J. N. Priestley, F. Seible, G. M. Calvi, *Seismic Design and Retrofit of Bridges*. New York: John Wiley & Sons Inc., 1996.

[14] M Bouchon, Effect of topography on surface motion. Bulletin of the Seismological Society of America, **63**, 615-632, 1973.

[15] D. W. Griffiths , and G. A. Bollinger, The effect of Appalachiam mountain topography on seismic waves. Bulletin of the Seismological Society of America, **69**, 1081-1105, 1979.

[16] D. Assimaki, G. Gazetas, Soil and topographic amplification on canyon banks and the Athens 1999 earthquake. Journal of Earthquake Engineering, 8(1), 1–44, 2004.

[17] GL Zhou, XJ Li, XJ Qi, Seismic response analysis of continuous rigid frame bridge considering canyon topography effects under incident SV waves. Earthquake Science, **23(1):** 53-61, 2010.

[18] HY Jia, DY Zhang, et al., Local site effects on a high-pier railway bridge under tridirectional spatial excitations: nonstationary stochastic analysis. Soil Dynamic and Earthquake Engineering, **52:** 55-69, 2013.

[19] JB Liu, YX Du, XL Du, et al., 3D Viscous-Spring artificial boundary in Time Domain. Earthquake Engineering and Engineering Vibration, **5(1)**: 93-102, 2006.

[20] JB Liu, YD Lu, A direct method for analysis of dynamic soil-structure interaction based on interface idea. CH Zhang and JP Wolf ed. *Dynamic Soil-Structure Interaction*, International Academic Publishers, 258-273, 1997.

[21] XL Du, *Theories and methods of wave motion for engineering*. Beijing: Science Press, 2009. (in Chinese)

[22] P. Kohnke. ANSYS theory reference-release 13.0. ANSYS Inc., 2010.